Supplementary Information for

AC needle-to-needle bare electrode discharge with nebulized sample injection for elemental analysis

Hao Yuan,[ab] Shu-Qi Li,[a] Jian-Ping Liang,*[a] Zhao-Lun Cui,[a] De-Zheng Yang*[a] and Rajdeep Singh Rawat[b]

[a] *Key Laboratory of Materials Modification by Laser, Ion, and Electron Beams (Dalian University of Technology), Ministry of Education, Dalian 116024, China*

[b] *Natural Sciences and Science Education, National Institute of Education, Nanyang Technological University, Singapore 637616 Singapore*

* Corresponding authors.

E-mail addresses: yangdz@dlut.edu.cn (D.-Z. Yang); liangjp@dlut.edu.cn (J.-P. Liang).

Calculation of rotational temperature and vibrational temperature

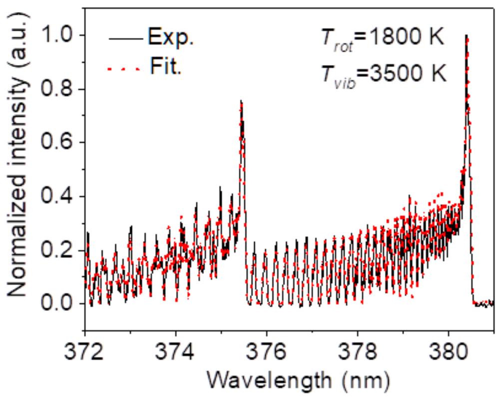

Fig. S1. Experimental (Exp.) and best-fitted (Fit.) spectral band of N_2 ($C^3\Pi_u$–$B^3\Pi_g$) for calculating T_{rot} and T_{vib}.

The rotational temperature (T_{rot}) and vibrational temperature (T_{vib}) of N_2 ($C^3\Pi_u$) can be calculated using "Specair" software,[1,2] under the assumption that the rotational states are in equilibrium and characterized by a Boltzmann distributio.[3] In the "Specair" software, a fitted N_2 ($C^3\Pi_u$–$B^3\Pi_g$) spectral band is generated by inputting a set of T_{rot} and T_{vib}. By comparing the fitted spectrum with the experimental one and iteratively adjusting T_{rot} and T_{vib} until the best-fitted spectrum is obtained, the corresponding temperatures under the experimental conditions can be determined. As an example, Fig. S1 shows the comparison of experimental and best-fitted curves of N_2 ($C^3\Pi_u$–$B^3\Pi_g$) emitted from needle-to-needle discharge, when the air is selected as the carrier gas. In this case, the corresponding T_{rot} and T_{vib} are 1800 K and 3500 K, respectively.

Calculation of electron density

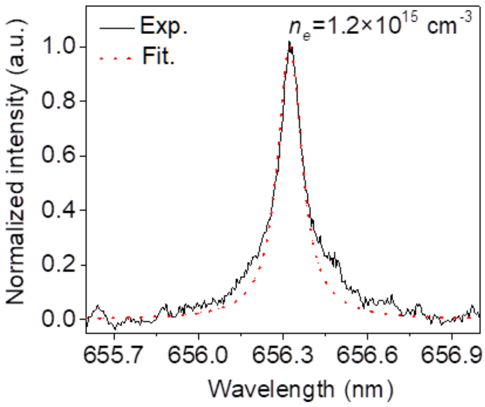

Fig. S2. Experimental (Exp.) and best-fitted (Fit.) spectral line of H_α for calculating electron density.

The electron density (n_e) of APDP can be calculated with the Stark broadening of H_α. The full wide at half maximum (FWHM) of spectral line of H_α ($\Delta\lambda$) can be calculated by the convolution of Gaussian profile ($\Delta\lambda_G$) and Lorentz profile ($\Delta\lambda_L$) as following:

$$\Delta\lambda = \sqrt{\Delta\lambda_G{}^2 + \left(\frac{\Delta\lambda_L}{2}\right)^2} + \frac{\Delta\lambda_L}{2} \text{ (nm).}$$ [4]

Among them, $\Delta\lambda_G$ is composed of Doppler broadening ($\Delta\lambda_D$), instrumental broadening ($\Delta\lambda_I$):

$$\Delta\lambda_G = \sqrt{\Delta\lambda_D{}^2 + \Delta\lambda_I{}^2} \text{ (nm).}$$ [5]

The $\Delta\lambda_I$ was measured by a low-pressure mercury lamp source in this study, which is 0.078 nm. And the $\Delta\lambda_D$ depends on T_g as following:

$$\Delta\lambda_D = 7.16 \times 10^{-7}\lambda\sqrt{\frac{T_g}{M}} \text{ (nm),}$$ [5]

where λ, and M are the central wavelength of H_α and the atomic mass of hydrogen, respectively.

For $\Delta\lambda_L$, it is composed of natural broadening ($\Delta\lambda_N$), resonance broadening ($\Delta\lambda_R$), van der Waals broadening ($\Delta\lambda_{vdW}$), and Stark broadening ($\Delta\lambda_S$):

$$\Delta\lambda_L = \Delta\lambda_N + \Delta\lambda_R + \Delta\lambda_{vdW} + \Delta\lambda_S \text{ (nm).}$$ [6]

Among them, $\Delta\lambda_N$ and $\Delta\lambda_R$ can be ignored in the conditions of this experiment, and $\Delta\lambda_{vdW}$ can be calculated as following:

$$\Delta\lambda_{vdW} = 2.42(T_g)^{-\frac{7}{10}} \text{ (nm).}$$ [7]

According to the above equations, the $\Delta\lambda_S$ is determined, and n_e can be calculated as the following equation:

$$n_e = 10^{17} \times \left(\frac{\Delta\lambda_S}{1.78}\right)^{1.5} \ (\mathrm{cm^{-3}}).$$ [8]

As an example, the calculation of n_e is illustrated in Fig. S2, with air as the carrier gas. In this case, $\Delta\lambda_S$ is 0.095 nm, and the corresponding n_e is 1.2×10^{15} $\mathrm{cm^{-3}}$.

Effects of experimental conditions on Cu SBR

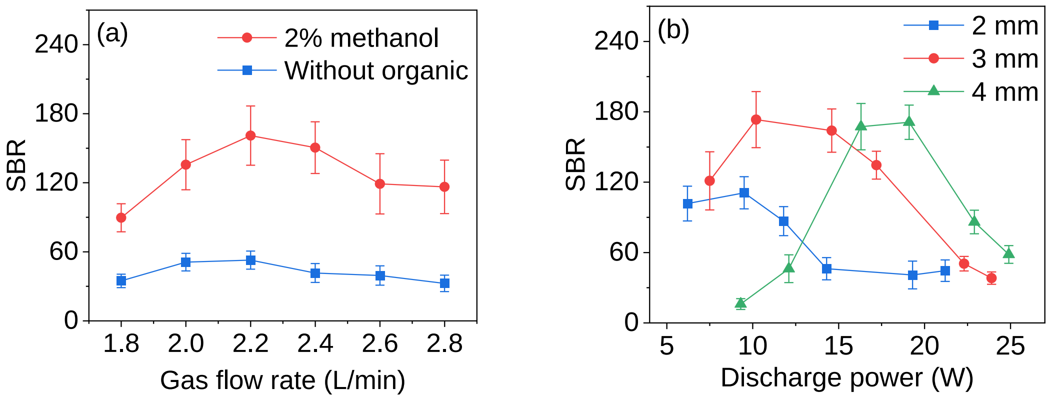

Fig. S3. (a) Cu SBR as a function of nebulizer gas flow rate with/without methanol in aqueous sample; (b) Cu SBR as a function of discharge power at discharge gaps of 2, 3, and 4 mm (error bars are the SDs of three measurements).

To investigate the applicability of the optimal conditions to other elements, the effects of nebulizer gas flow rate, methanol additive, discharge power, and discharge gap on Cu SBR were further examined. As shown in Fig. S3(a), the variation of Cu SBR with gas flow rate of nebulizer follows a trend similar with that of Ni SBR. The highest SBR for Cu and Ni are both observed with the gas flow rate of 2.2 L/min. Moreover, the addition of methanol in aqueous sample enhances Cu SBR by a factor of 2.9, also similar with its effect on nickel detection. As shown in Fig. S3(b), although the highest Cu SBR is achieved with 10.2 W discharge power at discharge gap of 3 mm, its value is close to that obtained at 14.6 W, which is the optimal power for nickel detection. Therefore, it is indicated that the optimal conditions established for nickel detection can also be applied to other elements.

Calibration curve for Ni, Cu, Cd, and Pb

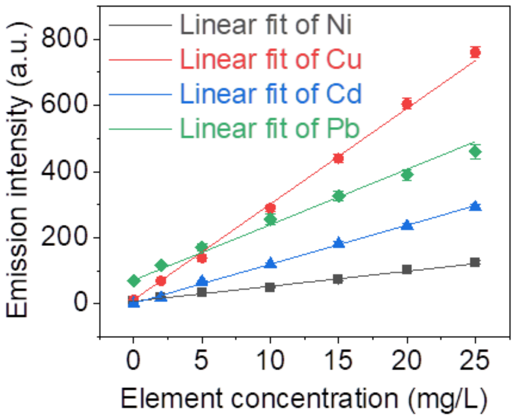

Fig. S4. Calibration curve of AC needle-to-needle bare electrode discharge with nebulized sample injection for detecting Ni, Cu, Cd, and Pb.

Stability of signal intensities

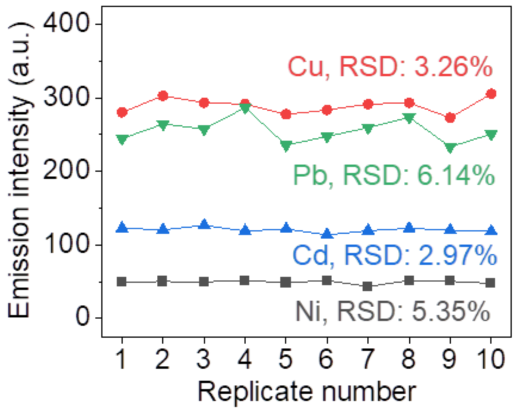

Fig. S5. Stability of emission intensities of Ni, Cu, Cd, and Pb in 10 times measurement.

References

1 C. O. Laux, T. G. Spence, C. H. Kruger and R. N. Zare, *Plasma Sources Sci. Technol.*, 2003, **12**(2), 125-138.

2 L. Yu, L. Pierrot, C. O. Laux and C. H. Kruger, *Plasma Chem. Plasma P.*, 2001, **21**(4), 483-503.

3 J. H. Kim, Y. H. Choi and Y. S. Hwang, *Phys. Plasmas*, 2006, **13**(9), 093501.

4 N. Konjević, M. Ivković and N. Sakan, *Spectrochim. Acta, Part B*, 2012, **76**, 16-26.

5 A. Y. Nikiforov, C. Leys, M. A. Gonzalez and J. L. Walsh, *Plasma Sources Sci. Technol.*, 2015, **24**(3), 034001.

6 M. A. Gigosos, *J. Phys. D: Appl. Phys.*, 2014, **47**(34), 343001.

7 S. Li, Y. Liu, H. Yuan, J. Liang, M. Zhang, Y. Li and D. Yang, *Appl. Sci.*, 2022, **12**, 8895.

8 M. A. Gigosos, M. Á. González and V. Cardeñoso, *Spectrochim. Acta, Part B*, 2003, **58**(8), 1489-1504.